Available online at www.sciencedirect.com
SCIENCE DIRECT®
Journal of Crystal Growth 260 (2004) 13–17
JOURNAL OF CRYSTAL GROWTH
www.elsevier.com/locate/jcrysgro

Photoluminescence study of InGaN/GaN quantum dots grown on passivated GaN surface

J.S. Huang[a,*], Z. Chen[a], X.D. Luo[a], Z.Y. Xu[a], W.K. Ge[b]

[a] *Institute of Semiconductors, Chinese Academy of Sciences, Beijing 100083, China*
[b] *Department of Physics, Hong Kong University of Science & Technology, Hong Kong, China*

Received 11 July 2003; accepted 6 August 2003
Communicated by M. Schieber

Abstract

We have measured photoluminescence (PL) and time-resolve photoluminescence (TRPL) from InGaN/GaN quantum dots (QDs) grown on passivated GaN surfaces by metalorganic chemical vapor deposition (MOCVD). Strong PL emission was observed from the QDs structure even at room temperature. By comparing the PL and TRPL dependence on temperature, a significant difference between the QD and wetting layer emissions was revealed. The QD emission is characterized by a strong exciton localization effect, which leads to a larger thermal activation energy, a nearly constant radiative lifetime independent of temperature and an unusual temperature behavior of the PL peak energy.

PACS: 78.55.Cr; 71.20.Nr; 78.55.−m; 39.30.+w

Keywords: A1. Atomic force microscopy; A1. Low dimensional structures; A3. Metalorganic chemical vapor deposition; B2. Semiconducting III–V materials

InGaN quantum dots (QDs) structure has attracted much attention for its potential application in low-threshold laser diodes (LDs) and superior performances due to its large localization effect [1–3]. Although it has been well recognized that the strong emission of the apparent InGaN quantum wells (QWs) originates from dot-like localized states caused by indium composition fluctuations [4], fabrication of an intentionally controlled QD structures in nitride semiconductors is still a big challenge. Hirayama et al. [5] reported their successful fabrication of self-assembled InGaN QDs on AlGaN surface by metalorganic chemical vapor deposition (MOCVD), using silicon as an anti-surfactant. While Tachibana et al. grew nano-scale InGaN self-assembled QDs on a GaN surface without any surfactant [6] and observed a room temperature lasing oscillation from their stacked QDs structure [1]. Fabrication of InGaN QDs using selective growth was also investigated by several groups [7–9]. More recently we have developed a new method to fabricate InGaN QDs by low-pressure MOCVD and observed a strong photoluminescence (PL) emission from the dots at room temperature [10]. In this

*Corresponding author. Fax: +86-10-82305056.
E-mail address: hjs@red.semi.ac.cn (J.S. Huang).

0022-0248/$ - see front matter © 2003 Elsevier B.V. All rights reserved.
doi:10.1016/j.jcrysgro.2003.08.008

paper, we further present the optical properties of InGaN/GaN QDs grown on a passivated GaN surface, an issue which has not been well exploited.

The InGaN/GaN QDs structure studied here was grown by low-pressure MOCVD on a passivated GaN substrate. Fig. 1(a) shows the schematic structure of the QD sample. A 30-nm-thick GaN buffer layer was first grown on a (0 0 0 1) sapphire substrate at 530°C, followed by 1-μm-thick high temperature (HT) GaN layer at grown 1030°C. Then the HT-GaN surface was passivated by oxygen in the atmosphere for 24 h and served as the substrate for the sequential growth of a GaN adjusting layer at 550°C. The passivation is expected to increase the energy barrier for hopping of the atoms, and the low-temperature growth decreases the surface diffusion length. All these factors would facilitate the formation of the nano-scale islands on the GaN surface, which is essential for the later-on InGaN QDs formation. The QDs structure contains four periods of InGaN/GaN (20/15 nm) layers grown at 850°C. The measured In composition is 0.15. For comparison, a reference sample of InGaN/GaN QW was grown separately. It has the same layered structure as the QD sample, but without the passivation process during growth (Fig. 1(b)). Details of the growth and characterization of the GaN adjusting layers were described elsewhere [10]. For surface morphology measurement, a third sample with only one InGaN layer was grown on a passivated LT-GaN surface. In the optical studies, time-resolved PL was performed under excitation of frequency-doubled ($\lambda = 360$ nm) laser pulses from a Ti:sapphire mode-locked laser and the signals were analyzed by a two-dimensional (2D) synchronous streak camera with an overall resolution of 15 ps. The PL measurement was carried out in cw configuration using a combination of a cooled GaAs PMT and a Jobin-Yvon Data-Link electronic system.

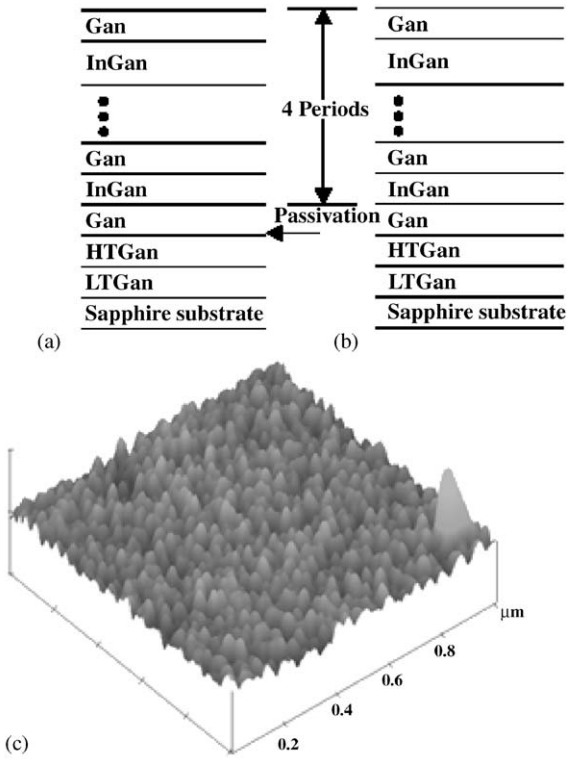

Fig. 1. (a) Schematic structure of InGaN/GaN QDs sample with passivated GaN surface; (b) QWs sample without passivated GaN surface and (c) AFM image of a single layer InGaN grown on passivated GaN surface.

Fig. 1(c) shows an atomic force microscope (AFM) image of the surface morphology of the third sample. It can be seen that the InGaN QDs were formed with an average size of 25 nm in diameter and 10-nm in height. The QDs density is estimated to be $10^{11}\,cm^{-2}$, higher than the commonly recognized density of dislocations ($2\times10^{10}\,cm^{-2}$) [11]. That is very important for good performance of optoelectronic devices.

Fig. 2(a) shows the PL spectrum of the InGaN/GaN QWs sample at 14 K. The PL is dominated by a 2D exciton emission peaked at 3.25 eV. Fig. 2(b) displays the PL spectra of the InGaN QDs sample at different temperatures ranging from 14 to 300 K. By comparing the PL spectra from the two samples, it is evident that a strong low-energy PL peak at 2.8 eV (see the 14 K PL in Fig. 2(b)) is an exciton emission of the QDs, while the high-energy emission around 3.15 eV is related to the wetting layer (WL) of the QD sample. The later corresponds to the 2D exciton emission in the QW sample. It is noticed that the PL energy of the reference sample is higher than that expected from its structure. This inconsistency is most likely due to the different indium incorporation in the

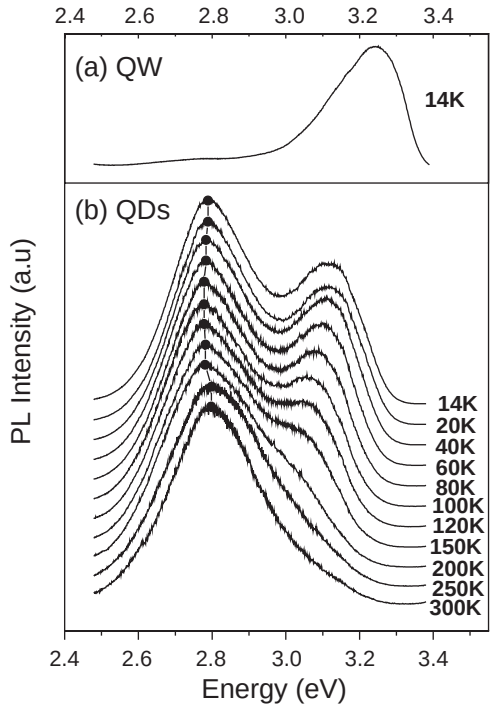

Fig. 2. (a) PL for the InGaN/GaN QWs sample at 14 K and (b) PL for the InGaN/GaN QDs sample at different temperature ranging from 14 to 300 K.

two growth procedures, which was found to be very sensitive to the growth conditions [12]. It is worth mentioning that the PL intensity of the QDs sample is more than 15 times higher than that of the QW sample at the same temperature of 14 K, showing a significantly improved luminescence efficiency in the QDs structure due to strong carrier localization.

As shown in Fig. 2(b), the intensity of the WL emission is comparable to that of the QDs at 14 K. This result presents a striking contrast to the case of InAs/GaAs QDs system, where the emission from WL is very weak due to efficient transfer of carriers from WL to QDs even at low temperatures. For the InGaN/GaN QD case, the relatively higher PL intensity from WL at low temperature can be attributed to a larger exciton bind energy in the InGaN system, as will be discussed later. When temperature increases, the PL intensity of the WL decreases much faster than that of the QDs, leading to an increase of the relative PL intensity of the QDs. The QD emission remains intense even at room temperature, in consistent with the strong carrier localization in QDs due to a 3D carrier confinement.

Fig. 3 presents the temperature dependence of the PL peak energy for the WL (a) and QDs (b), respectively, in the QDs sample. It is clear that the energy variation with temperature is quite different for the two cases. For the WL the photon energy follows the band gap very closely below 200 K. This behavior is very similar to that observed in 2D InGaN/GaN QWs (not shown). The fitting of the experimental data with Varshini empirical formula yields Varshini parameters of $\alpha = 1.07$ meV/K and $\beta = 173.3$ K, which are comparable to what we obtained in our QW sample. For the QD emission, however, the photon energy decreases first, but then increases with increasing

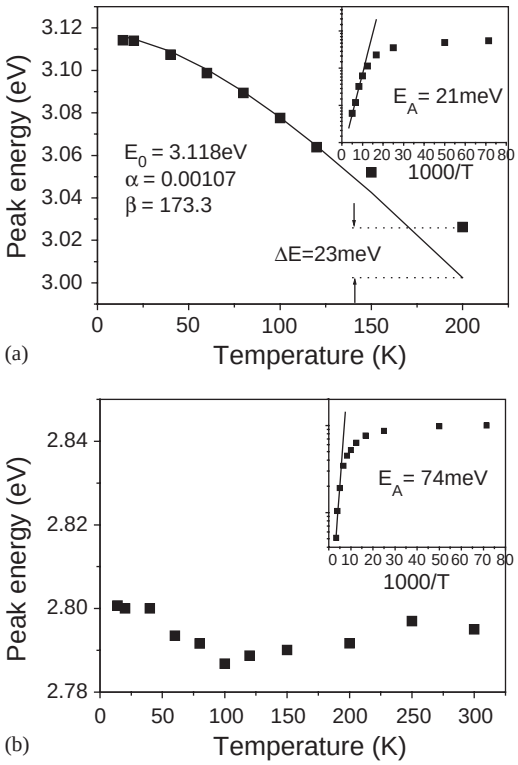

Fig. 3. PL peak energy vs. temperature for both (a) WL emission and (b) QDs emission in the QDs sample. The solid line in Fig. 3(a) is the fitting of the data using the same Varshini parameters as in the QWs sample. The insets are Arrhenius plot for the WL and QDs emissions.

temperature, showing an S-shaped behavior of the PL energy. This unusual temperature dependence is a typical characteristic of self-organized QDs [13], resulting from the thermal activation and transfer of excitons localized at different potential minima caused by the size distribution of QDs. Note that the overall variation of the photon energy is not large. The reduced red shift observed for the QD structures can be partly explained by a partial decoupling of the phonon–exciton interaction of the QDs [14,15].

The integrated PL intensity vs. temperature is plotted in the insets of Fig. 3 for both QD and WL emissions. The experimental data are fitted using $I(\mathrm{T}) = I_0/[1 + C\exp(-E_0/kT)]$. The thermal activation energy E_0 can be obtained from the data fitting. The thermal activation energy for the WL emission is 21 meV, in good agreement with the value of 23 meV, an energy deviation from the expected value according to the Varshini relation between the PL peak energy and temperature (see Fig. 3(a)). This deviation has been regarded as a transition of localized exciton to delocalized exciton emissions, and therefore the corresponding energy deviation is often taken as a measure of the exciton localization energy [14]. The thermal activation energy of the QD emission is estimated to be 74 meV, much larger than that for the WL. A large activation energy of the QDs efficiently prevents carriers from thermal quenching and ensures strong emission up to room temperature. It explains the increase of the relative PL intensity of the QD with the increase of temperature. We note that the value of 74 meV is far less than the energy difference between the QDs and the WL emissions. It can then be postulated that the decrease of the QD PL intensity is due to the thermal activation of the non-radiative recombination centers as often observed in many semiconductors, rather than the evaporation of the carriers from the QDs to the WL.

To further study the dimensional property of the QD structure, we have studied radiative and non-radiative recombination dynamics of the InGaN/GaN QD sample by combining the PL and time-resolved PL results. The values of the radiative lifetime τ_{rad} and non-radiative lifetime τ_{nonrad} are deduced from the PL decay time(τ_{PL}) and the PL intensity as a function of temperature using the relation $\eta_{\mathrm{int}} = 1/(1 + \tau_{\mathrm{rad}}/\tau_{\mathrm{nonrad}})$, where η_{int} is an internal quantum efficiency. To make it simple, η_{int} is set to be unity at low temperature, since the non-radiative recombination centers are usually frozen up and the radiative recombination dominates the PL at low temperature. Then, τ_{rad} and τ_{nonrad} can be expressed as a functions of the measured decay time τ_{PL}.

$$\tau_{\mathrm{rad}}(T) = \frac{I(14\,\mathrm{K})}{I(T)}\,\tau_{\mathrm{PL}}(T), \tag{1}$$

$$\tau_{\mathrm{nonrad}}(T) = \frac{I(14\,\mathrm{K})}{I(14\,K) - I(T)}\,\tau_{\mathrm{PL}}(T). \tag{2}$$

In Fig. 4, the deduced τ_{rad} and τ_{nonrad} for the WL and QDs emissions are plotted as a function of temperature. It can be seen that there is no significant variation of τ_{rad} from 14 to 200 K for the QDs emission, showing a characteristic behavior of the 0D excitons. Whereas τ_{rad} for the WL increase linearly with increasing temperature when $T > 100$ K, in consistence with the well-known theoretical prediction in a 2D system [16].

In conclusion, the optical properties of InGaN/GaN QDs grown on passivated GaN surfaces by

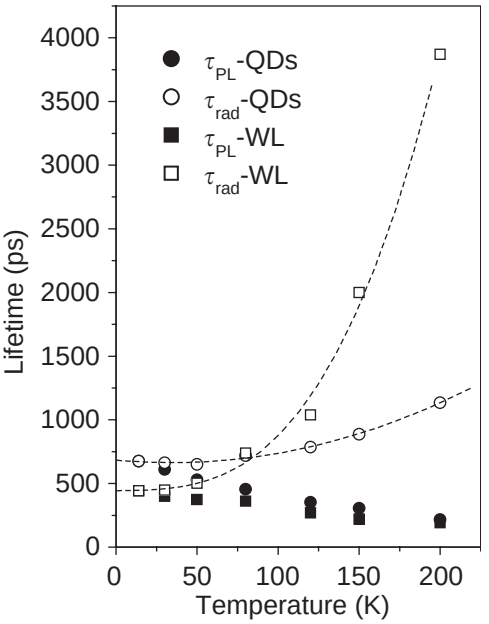

Fig. 4. PL decay time and radiative lifetime for the emissions from WL and QDs.

MOCVD are studied by PL and time-resolve photoluminescence (TRPL). By comparing temperature dependence of PL and TRPL, a significant difference between the QD and WL emissions was observed. The QD emission is characterized by a strong exciton localization effect, which leads to a larger thermal activation energy, a nearly none variation of the radiative lifetime with temperature, and an unusual temperature behavior of the PL peak energy.

This work was supported by the special funds for Major State Basic Research Project No. G001CB3095, No.G2000683 of China, Grant No.10274081 from NSFC and Grant HKUST 6076/02P.

References

[1] Koichi Tachibana, Takao Someya, Yasuhiko Arakawa, Appl. Phys. Lett. 75 (1999) 2605.
[2] J. Zhang, M. Hao, P. Li, S.J. Chua, Appl. Phys. Lett. 80 (2002) 485.
[3] Hideki Hirayama, Satoru Tanaka, Peter Ramvall, Yoshinobu Aoyagi, Appl. Phys. Lett. 72 (1998) 1736.
[4] Y. Narukawa, Y. Kawakami, M. Funato, S. Fujita, S. Fujita, S. Nakamura, Appl. Phys. Lett. 70 (1997) 981.
[5] Hideki Hirayama, Satoru Tanaka, Peter Ramvall, Yoshinobu Aoyagi, Appl. Phys. Lett. 72 (1998) 1736.
[6] K. Tachibana, T. Someya, Y. Arakawa, Appl. Phys. Lett. 74 (1999) 383.
[7] J. Wang, M. Nozaki, M. Lachab, Y. Ishikawa, R.S. Qhalid Fareed, T. Wang, M. Hao, S. Sakai, Appl. Phys. Lett. 75 (1999) 950.
[8] Koichi Tachibana, Takao Someya, Satomi Ishida, Yasuhiko Arakawa, Appl. Phys. Lett. 76 (2000) 3212.
[9] D. Kapolnek, S. Keller, R.D. Underwood, S.P. DenBaars, U.K. Mishra, J. Crystal Growth 189 (1998) 83.
[10] Zhen Chen, Dacheng Lu, Hairong Yuan, Peide Han, Xianglin Liu, Yufeng Li, Xiaohui Wang, Yuan Lu, Zhanguo Wang, J. Crystal Growth 235 (2002) 188.
[11] B. Damilano, N. Grandjean, F. Semond, J. Massies, M. Leroux, Appl. Phys. Lett. 75 (1999) 962.
[12] N. Grandjean, J. Massies, Appl. Phys. Lett. 72 (1998) 1078.
[13] Z.Y. Xu, Z.D. Lu, X.P. Yang, Z.L. Yuan, B.Z. Zheng, J.Z. Xu, Phys. Rev. B. 54 (16) (1996) 11528.
[14] S. Chichibu, T. Azuhata, T. Sota, S. Nakamura, Appl. Phys. Lett. 70 (1997) 2822.
[15] M. Grundmann, J. Christen, N.N. Ledentsov, J. Bohrer, D. Bimberg, Phys. Rev. Lett. 74 (1995) 4043.
[16] J. Feldmann, G. Peter, E.O. Göbel, P. Dawson, K. Moore, C. Foxon, Phys. Rev. Lett. 59 (1987) 2337.